Sensors & Transducers, Vol. 220, Issue 2, February 2018, pp. 9-19

www.sensorsportal.com

Sensors & Transducers

Published by IFSA Publishing, S. L., 2018
http://www.sensorsportal.com

Differences in VOC-Metabolite Profiles of *Pseudogymnoascus destructans* and Related Fungi by Electronic-nose/GC Analyses of Headspace Volatiles Derived from Axenic Cultures

[1] Alphus Dan WILSON and [2] Lisa Beth FORSE

[1] Forest Insect and Disease Research, USDA Forest Service, Southern Hardwoods Laboratory, 432 Stoneville Road, Stoneville, MS, 38776-0227, USA

[2] Center for Bottomland Hardwoods Research, Southern Hardwoods Laboratory, 432 Stoneville Road, Stoneville, MS, 38776-0227, USA

[1] Tel.: (+1)662-686-3180, fax: (+1)662-686-3195

E-mail: dwilson02@fs.fed.us

Received: 10 November 2017 /Accepted: 5 February 2018 /Published: 28 February 2018

Abstract: The most important disease affecting hibernating bats in North America is White-nose syndrome (WNS), caused by the psychrophilic fungal dermatophyte *Pseudogymnoascus destructans*. The identification of dermatophytic fungi, present on the skins of cave-dwelling bat species, is necessary to distinguish between pathogenic (disease-causing) microbes from those that are innocuous. This distinction is an important step for the early detection and identification of microbial pathogens on bat skin prior to the initiation of disease and symptom development, for the discrimination between specific microbial species interacting on the skins of hibernating bats, and for early indications of potential WNS-disease development based on inoculum potential. Early detection of *P. destructans* infections of WNS-susceptible bats, prior to symptom development, is essential to provide effective early treatments of WNS-diseased bats which could significantly improve their chances of survival and recovery. Current diagnostic methods using quantitative polymerase chain reaction (qPCR) for the targeted detection of specific fungal pathogens on bats require semi-invasive methods (skin swabs) that tend to arouse hibernating bats resulting in consumption of valuable fat reserves that reduce their chances of winter survival. Also, qPCR only indicates the presence and quantity (fungal loads) of specific fungal inoculum on bat skin, but does not conclusively indicate that the fungus has infected the host, or that a disease state exists, since template fungal DNA used for PCR comes from outside of the host rather than from within the host. Consequently, we are developing non-invasive methods for the early detection of WNS-disease based on the production of unique mixtures of volatile organic metabolites detected in sampled air (in proximity to bats) using a dual-technology, electronic-nose/gas chromatography device. This approach initially was tested in the current study to evaluate the potential of e-nose tools for identifying and discriminating between complex mixtures of volatile fungal metabolites produced by five *Pseudogymnoascus* species in pure cultures. We determined that the Heracles II e-nose system was effective in discriminating between *P. destructans* and related *Pseudogymnoascus* species using principal component analysis (PCA) of smellprints signatures coupled with discrimination index (DI) and GC-patterns of major VOC-peaks produced from analysis of aroma profiles of volatile metabolites in culture headspace.

Keywords: Electronic aroma detection, E-nose, Fungal metabolites, Gas chromatography, Noninvasive early disease diagnosis, Volatile organic compounds, White-nose syndrome.

1. Introduction

A diverse range of microbes have been isolated from the skins of cave-dwelling bats [1, 2]. Skin swabs taken from small mammalian trogloxenes (animals that are temporary cave residents and move freely in and out of caves), particularly insectivorous bats while in hibernation, is a common means by which animal pathologists and wildlife researchers obtain cultures and conduct diagnostic tests such as polymerase chain reaction (PCR) for determining the possible etiology of various dermatophytic diseases acquired by volant mammals.

Cave-dwelling bats are attacked by relatively few fungal dermatophytes including *Pseudogymnoascus destructans* (Pd), causing deep-seated skin infections, and *Trichophyton redellii* (ringworm) that causes only superficial skin infections [3]. White-nose Syndrome (WNS), caused by the psychrophilic dermatophyte and pervasive nonnative (exotic) fungal pathogen (*P. destructans*), has emerged over the past decade as the most important disease of cave-dwelling bats in North America. This disease has caused extensive mortality and regional population declines of hibernating bat species in the eastern, mid-western and southern United States as well as southeastern Canadian provinces [4]. WNS is known to significantly affect at least eight species of bats in North America [5-7].

The capability of wildlife disease diagnosticians to detect the presence of pathogenic microbes growing on the skins of bats and determine the early onset of dermatophytic diseases is a critical need for achieving early WNS-disease detection, so essential for the implementation of control treatments at early stages of bat hibernation before WNS-disease causes significant damage to bat hosts. However, taking skin swabs from bats during hibernation, either for PCR and DNA-sequencing or for other purposes, often arouses bats from torpor, causing unnecessary consumption of fat reserves and physiological stress that threatens their winter survival. To address this problem, we are developing noninvasive electronic-nose technologies as new diagnostic tools to chemically detect and identify pathogenic microbes and disease, particularly *P. destructans* that causes WNS during winter bat hibernation within caves and other hibernacula.

Electronic-nose (e-nose) devices previously have been used extensively to identify microbial pathogens in culture and detect diseases of plants, animals, and humans [8, 9]. E-nose devices are particularly useful as diagnostic tools for the discrimination of complex gaseous mixtures of volatile organic compounds (VOCs), produced as metabolic products of microbes, released into the headspace of microbial cultures [10, 11]. Some important potential advantages of using e-nose devices as diagnostic tools, particularly for hibernating bats, are noninvasive early detection of infectious diseases and causal agents (minimal disruption of bat torpor patterns and behavioral disturbances during hibernation), rapid real-time disease detection capabilities using portable e-nose devices, low-cost diagnostic testing, high precision of measurements, low incidence of false positive results, and complex VOC-mixture detections without the need to identify individual chemical species within diagnostic samples [12, 13].

Soil-borne psychrophilic (cold-loving) fungi, related to the WNS Pd-pathogen (*P. destructans*), include various other *Pseudogymnoascus* species (such as *P. appendiculatus*, *P. roseus*, and *P. verrucosus*), and numerous other *Geomyces* species. *Pseudogymnoascus pannorum* var. *pannorum* occasionally causes superficial human diseases as a nonaggressive, dermatophytic pathogen [14, 15]. Although these fungi have similar metabolisms, differences in specific metabolic pathways used by these microbes result in the production and release of different types, combinations, quantities, and mixtures of fungal VOCs into the headspace of axenic cultures. Consequently, the production of complex, unique headspace VOC-metabolite mixtures may be used as a basis to discriminate between microbial species when analyzed using specialized gas multi-sensor arrays such as e-nose devices [8]. Likewise, knowledge of differences in VOC-metabolites produced by fungi may be applied to electronic-nose detection of fungal pathogens growing on bat skins, and the subsequent early noninvasive detection of dermatophyte diseases when these fungi penetrate the skin of bat hosts and initiate pathogenesis, generating additional abnormal disease-biomarker VOCs [16, 17].

The purpose of this study was to examine chemical differences in the VOC-metabolite profiles of *Pseudogymnascus destructans* and four other genetically-related *Pseudogymnoascus* species based on the production of unique mixtures of headspace volatiles in culture as determined by simultaneous analyses utilizing a dual-technology, electronic-nose and gas chromatography device. The specific objectives were to: 1) determine differences in the chemical composition of headspace volatile (metabolite) mixtures revealed by dual-column gas chromatographic peak patterns, 2) document differences in electronic-nose signature (smellprint) patterns derived from an e-nose multi-sensor array, and 3) develop a 3-D aroma e-nose map of culture headspace VOCs from *Pseudogymnoascus* species with supporting chemical-relatedness data based on 3-dimensional principal component analysis (PCA). A previous related study of volatile metabolites, produced by *Pseudogymnoascus* species compared to genetically-related *Geomyces* species, provided earlier indications of chemical relatedness and differences between the headspace VOC-metabolites based on similar analyses performed with the Heracles II fast gas chromatograph (GC)/e-nose combination-technology instrument [18].

2. Materials and Methods

The *Pseudogymnoascus* species, selected for e-nose and GC-chemical analysis in this study, are

a group of genetically-related fungi isolated from a wide diversity of physical environments with different types of carbon substrates and growth conditions.

2.1. Fungal Strains and Growth Conditions

Five *Pseudogymnoascus* species were tested in this study including: *Pseudogymnoascus destructans* 20631-21 (PD6), the ATCC type strain originally isolated from a little brown bat (*Myotis lucifugus*) at Williams Hotel Mine, New York; *Pseudogymnoascus destructans* M-3902 (PD3) from West Virginia; *Pseudogymnoascus appendiculatus* UAMH-10509 (PA1) and *Pseudogymnoascus verrucosus* UAMH-10579 (PV1), both isolated from a *Sphagnum fuscum-Picea mariana* bog near Alberta, Canada; *Pseudogymnoascus roseus* 722101 (PR1), the type strain of the genus [19]; and *Pseudogymnoascus pannorum* var. *pannorum* CMF-2582 (GP8). Three additional *P. destructans* strains were used for only GC analyses of VOC-metabolite headspace volatiles. All *Pseudogymnoascus* isolates were obtained from the Center for Forest Mycology Research (CFMR; Madison, WI). Growth media were sterilized at 121 °C under 15 PSI for 20-40 minutes. For long-term storage at −80 °C, strains were grown and maintained in 24 hour darkness on Sabouraud dextrose agar (SDA) (4 % dextrose, 1 % Neopeptone, 2% agar), incubated at 14°C for 8 weeks. Asexual spores were collected by washing sporulating SDA cultures with 5 ml of 0.1% deoctylsulfosuccinate (DSS) in SD broth to which an equal volume of 50% glycerol was added to suspend hydrophobic conidia [20].

2.2. Pre-run Sample Preparation Procedures

All fungal strains tested were grown on SDA slants in 100 mL Kimax GL45 glass bottles with 40 mL SDA culture medium per bottle. Five glass-bottle cultures were prepared as replications for each strain. Three bottles of uninoculated SDA slants (SAB) served as controls. Two samplings of headspace volatiles from each replicate bottle were analyzed by withdrawing gas samples through Pyrex PTFE-faced silicone rubber septa secured with GL45 PBT open-top screw caps. Agar slants were inoculated with 20 µl of frozen conidial spore suspension, spread with a sterile glass rod. Cultures were grown in darkness at 14 °C for 4 weeks. To allow headspace VOCs to accumulate, cultures were moved to room temperature at 21 °C in the dark for 18 hours prior to analysis on a weekly basis. The total quantity of VOCs accumulating in culture headspace over each weekly period were largely removed from bottle cultures for analysis each week so that the quantity of VOCs analyzed weekly indicated the quantity that had accumulated only over a one-week period.

An analytical reference standard custom mixture (Restek, Bellefonte, PA, product number 561203), composed of 11 sequential aliphatic alkanes (C_7–C_{17}), was utilized prior to all GC sample analyses to set up Kovats calibrations for determinations of Kovats Retention Indexes for specific peaks of VOC-metabolites (KRI-v) present in sample headspace, and for tentative compounds (KRI-t) indicated as potential identifications of peak compounds, based on the nearest matches of KRI-values from among >83,000 compounds present in the Kovats indices reference library. In addition, Relevance Index (RI) values, indicating percentage probability of identity match, based on Kovats values for specific compounds, was selected to be displayed with GC-output data in association with KRI-t values of each tentative identity compound.

2.3. Instrument Configuration Parameters

The Heracles II GC/Electronic-nose system (Alpha MOS, Toulouse, France), composed of a dual-column (DB-5 and DB-1701) fast-gas chromatograph (GC) with hydrogen carrier gas, flame-ionization detectors (FID) and multiple e-nose sensors, was utilized for all culture VOC-headspace analyses. Operational gases (hydrogen carrier and oxygen for FID detectors) were generated using an Alliance Desktop Hydrogen Generator system PAR.H2.180.V3 (MicroProgel Srl, Torreglia, Italy).

Fungal VOC-metabolites were manually injected using 15 ml of culture headspace per sample via 20 cc (Cadence Science Inc., Cranston, RI) glass syringe, Peltier-cooled adsorption cold trapped at 30 °C for 50 s before split-injection at 10 ml/min into 10 m, 0.18 mm-diam. DB-5 and DB-1701 GC columns following isothermal heating at 240 °C for 30 s at 57 kPa of pressure. Analyses were conducted at an initial oven temperature of 50 °C, ramping at 1 °C/s up to 80 °C, then accelerating the heating rate to 3 °C/s up to 250 °C for 21 s. Analyzer injection volume was set at 5000 µl at a speed of 125 µl/s, injection temperature of 200 °C at 10 kPa pressure, injection time 45 s, and venting at 30 ml/min. The two FID detector temperatures, for separate dual columns, were set at 260 °C. Retention times (RTs) of VOCs from each sample type were recorded for each peak for both GC columns. Dual-column data outputs provided opportunities to help resolve VOC-peaks that had close or overlapping RTs.

GC-output data also included the range of VOC peak heights for all sample types and replications. Peak area was not used due to small widths of VOC-analyte peaks. Actual quantities of VOCs present in individual peaks also were not determined since quantitative standard curves using analytical standards for specific compounds were not yet established.

The e-nose analyzer component of the dual-technology Heracles II system utilizes a very large number of proprietary metal oxide semiconductor (MOS) sensors in the sensor array. For data analyses involving statistical discrimination algorithms, only

those sensors in the array that provided the largest output responses that added significantly to sample discriminations were utilized in data analyses, such as for PCA plots and derivations of aroma signatures or smellprint patterns that define the unique aroma fingerprints of VOC-metabolite mixtures contained within fungal headspace volatiles. Statistical analyses were carried out using Alphasoft V14.20 and AroChembase software.

2.4. Data Acquisition Parameters

Data acquisition rates for both GC data recording and e-nose data from the sensor array were collected every 0.01 s intervals (100 data points per second) set at a constant data-recording rate for the entire duration of each analysis run. Total run time for all analysis runs was 110 s. Both dual GC-columns and e-nose sensor arrays were purged with ultrapure air or blank samples between each sample analysis run to prevent carryover of VOC sample-analytes between runs.

2.5. Principal Component Analysis

Three-dimensional principal component analysis (PCA) was performed on e-nose data using Heracles II software to compare the relatedness between aroma signature patterns derived from e-nose sensor array output responses to fungal VOC-metabolite mixtures in culture headspace. Distances between centers of data clusters (PCA mapping distance), derived from sensor array outputs of each fungal culture headspace (aroma classes or sample type), were determined on a PCA plot or aroma map by pairwise comparisons of aroma classes (VOC headspace sample types) in all possible combinations along with aroma Pattern Discrimination Index (PDI), expressed as a percentage approximating the statistical level of discrimination (P-values) between corresponding sample types compared, based on calculated differences in aroma signature patterns (smellprints).

3. Results

3.1. Gas Chromatographic Analysis

Analyses of gaseous VOC-mixtures produced by individual fungi in SDA-culture headspace, based on gas chromatographic (GC) patterns recorded on chromatograms, provided indications of differences in the types, atomic weights, and quantities of volatile metabolites produced. All five *Pseudogymnoascus* species appeared to produce common or similar VOC-metabolite peaks in the 16.33-16.50 s RT-range in 3-week old cultures. All species, except for *P. pannorum* var. *pannorum*, also produced an additional peak at a RT of 26.57 s, although *P. destructans* strains did not produce the 26.57 peak until several months later in older cultures. The human pathogenic strain of *P. pannorum* var. *pannorum* produced two unique VOC-metabolites at RTs of 15.30 and 59.60 which distinguished this species from the others.

Additional GC-analyses of headspace volatile metabolites, produced by five strains of *P. destructans* in 2-week old SDA-cultures, provided indications of tentative identities for ten primary peaks recorded in GC chromatographs based on RTs and KRI-values of sample metabolites compared to those of known compounds in the AroChemBase Kovats reference library (Table 1). Calculations of RI-values for each known compound relative to sample VOCs provided indications of probability ranges for compound-identity matches. Compounds represented by peaks 2, 5, and 10 were the largest metabolic components (quantitatively) among the VOCs present in the Pd headspace samples from SDA axenic cultures. The Pd-VOC indicated by peak 10 was the most abundant compound produced by all Pd-strains tested on SDA-medium. The tentative identities of VOC-metabolites produced by Pd strains indicated major components consisting of monoterpene and aliphatic aldehyde chemical classes. The tentative identities of minor Pd VOC-metabolites possibly include aliphatic alkanes, carboxylic acids, methyl esters, lactones, ketones, aromatic hydroxides and furans (Table 1).

3.2. E-nose VOC-Signature Patterns

Differences in e-nose smellprint patterns, derived from multisensor e-nose array outputs of the Heracles II GC/electronic-nose instrument, provided additional data for discriminations between *Pseudogymnoascus* species based on differences in e-nose multisensor responses to unique VOC-metabolite mixtures produced in SDA-culture headspaces. The e-nose smellprints, produced by the e-nose multisensor array in response to differences in VOC-metabolite mixtures, were significantly different from that of SDA-medium that served as a control for comparisons to indicate the smellprint of background VOCs released from the common SDA culture medium itself used in all sampling bottles (Fig. 1, A-F).

The sensor numbers, labeled on the x-axis, are listed in the same order for all sample types analyzed. All of the smellprints, produced as sensor-array responses to VOC headspace volatiles of fungi in culture, varied considerably in sensor response intensity, shown on the y-axis, and in overall smellprint patterns (profiles) compared with each other and with the SDA-control (Fig. 1F). The smellprint pattern of *P. appendiculatus* differed quite drastically from the other *Pseudogymnoascus* species, including the WNS fungal pathogen (*P. destructans*), *P. pannorum* var. *pannorum*, *P. roseus*, and *P. verrucosus* (Fig. 1 A-E). The smellprint pattern of *P. roseus* only superficially resembled that of *P. verrucosus* strains, but differences in individual sensor intensities and responses varied considerably (Fig. 1 D, E).

Table 1. Gas chromatographic data indicating tentative identities of VOC-metabolite compounds produced by *Pseudogymnoascus destructans* strains in SDA-culture headspace.

Peak	RT[a]	KRI-v[b]	Peak heights	VOC identity	KRI-t[c]	RI range[d]	Chemical class
1	13.58	409	3,888 – 4,471	Trimethylamine	425	64.40 – 70.34	Tertiary amine
				Methyl formate	401	2.25 – 30.87	Methyl ester
2	16.33	473	9,216 – 32,580	Propanal	499	68.61 – 72.67	Aliphatic aldehyde
				Propenal	450	59.51 – 63.56	Aliphatic aldehyde
3	17.81	507	2,387 – 2,897	Furan	502	14.72 – 92.06	Furan
				Pentane	500	18.67 – 39.43	Alkane
4	21.20	584	3,230 – 6,944	Butane-2,3-dione	589	84.40 – 89.74	Diketone
				Butan-2-one	594	79.40 – 84.74	Ketone
5	26.18	650	1,463 – 28,861	2-butenal	646	81.69 – 90.09	Aldehyde
				3-methylbutanal	652	69.88 – 77.79	Aldehyde
6	49.82	875	5,234 – 10,638	2-methylbutanoic acid	872	28.25 – 85.86	Carboxylic acid
				3-methylbutanoic acid	862	16.98 – 74.01	Carboxylic acid
7	58.83	980	5,251 – 11,719	Phenol	986	88.20 – 91.50	Aromatic hydroxide
				δ-valerolactone	961	50.15 – 50.85	Lactone
8	60.47	1001	1,872 – 4,195	Myrcene	996	68.29 – 88.62	Monoterpene
				α-phellandrene	1004	67.17 – 85.72	Cyclic monoterpene
				β-pinene	992	77.55 – 84.83	Bicyclic monoterpene
9	61.09	1010	2,475 – 7,581	α-phellandrene	1004	84.56 – 90.72	Cyclic monoterpene
				(+)-α-phellandrene	1006	83.83 – 89.99	Cyclic monoterpene
10	62.94	1038	21,081 – 94,008	β-phellandrene	1031	69.68 – 90.31	Cyclic monoterpene
				Limonene	1030	71.68 – 88.98	Cyclic monoterpene

[a] RT = Retention Times (seconds) for VOC-metabolite compounds run within a 10 m DB-5 column using the GC run parameters specified previously and derived from headspace samples collected from two-week old cultures from five Pd-strains with three replications for each.
[b] KRI-v = Kovats Retention Index for specific volatile-metabolites present in headspace samples run with a 10 m DB-5 column using 11-alkane (C_7-C_{17}) analytical reference standard calibration.
[c] KRI-t = Kovats Retention Index for tentative compounds indicated as potential identity based on close KRI-values.
[d] RI = Relevance Index, indicating percentage probability of identity match, based on Kovats values for specific compounds run with a 10 m DB-5 column.

The aroma signature pattern (smellprints) of SDA-culture headspace VOC-metabolite mixtures from *P. destructans* strains was unique in having only six major sensors that responded to VOCs while all other sensors in the array had very minimal responses to Pd-volatile metabolites (Fig. 1 B). The smellprints of *P. roseus* and *P. verrucosus* strains also exhibited six major sensor responses, but both species had somewhat stronger minor sensor responses with different patterns and intensities.

The sensor-response patterns of *P. roseus* and *P. verrucosus* strains also showed very little resemblance to the smellprint patterns of *P. appendiculatus* and *P. pannorum* var. *pannorum.* None of the smellprints of the five *Pseudogymnoascus* species showed any resemblance or similarities in patterns with SDA-controls for major and minor sensor responses that occurred at much lower sensor intensities due to the absence of any fungal VOC-metabolites (Fig. 1 F).

3.3. Principal Component Analysis

The differences observed in sensor responses of the Heracles II e-nose sensor array to complex gaseous mixtures of volatile metabolites released into culture headspace were analyzed statistically using principal component analysis (PCA) to measure and quantify the differences between e-nose aroma signatures produced by individual fungi.

Pairwise comparisons of e-nose aroma profiles of *Pseudogymnoascus* species, tested in all possible combinations to assess and measure these differences, indicated widely varying PCA mapping distances (between data clusters and smellprint signatures for individual fungal species) and statistical differences as measured using a percentage Pattern Discrimination Index (PDI) for each pairwise comparison (Table 2). These analyses collectively included twenty-one distinct PCA-pairwise comparisons between individual strains of each fungal species and between

the fungal strains and uninoculated SDA slant (SAB) controls.

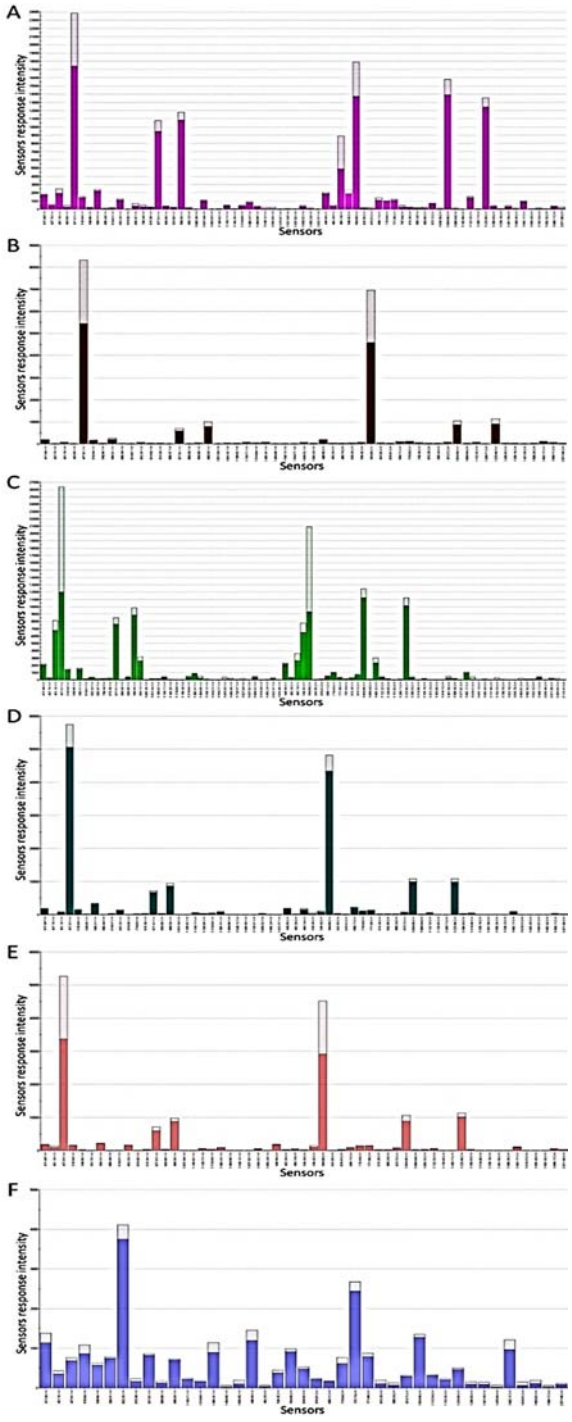

Fig. 1. E-nose aroma-signature patterns (smellprints) of complex headspace volatile mixtures, composed of fungal VOC-metabolites derived from five *Pseudogymnoascus* species in SDA-cultures. Smellprint signatures, composed of output patterns from the e-nose sensor array, include: A) *P. appendiculatus*, B) *P. destructans* (the WNS Pd-pathogen), C) *P. pannorum* var. *pannorum*, D) *P. roseus*, E) *P. verrucosus*, F) SDA-medium control.

Strains of all five *Pseudogymnoascus* species tested showed high levels of significant differences from SDA-culture medium controls, in terms of PCA mapping distances (range of 9,467-106,723 mapping units), percentage PDI (range of 72.3-98.7 %) and aroma signatures.

Table 2. Chemical differences between electronic-nose VOC-profiles of five *Pseudogymnoascus* species based on SDA-culture headspace volatiles analyzed by 3-D principal component analysis with pattern discrimination index.

Class 1	Class 2	PCA distance[a]	PDI (%)[b]
PA1	PD3	82,334.10	84.94
	PD6	28,688.58	46.70
	PP8	21,517.88	76.88
	PR1	43,728.52	91.98
	PV1	9,466.80	22.49
	SDA	33,558.06	88.32
PD3	PD6	55,673.80	61.93
	PP8	101,318.45	90.28
	PR1	38,967.67	57.28
	PV1	81,088.75	83.76
	SDA	106,723.11	89.36
PD6	PP8	46,643.56	72.09
	PR1	17,424.10	25.88
	PV1	25,798.87	39.68
	SDA	51,724.00	72.25
PP8	PR1	62,777.83	98.26
	PV1	22,026.64	69.63
	SDA	21,992.46	94.65
PR1	PV1	42,352.60	88.24
	SDA	68,801.81	98.71
PV1	SDA	29,460.40	78.39

[a] PCA distances indicate actual mapping distances between data clusters of sample types determined from aroma signatures.

[b] Pattern Discrimination Index (DPI) values indicate percentage differences in VOC-metabolite aroma profiles by pairwise comparisons of sample types based on PCA tests of aroma signature (smellprint) patterns derived from the e-nose sensor array.

PDI results provided precise numerical values (percentage indications) of chemical differences between aroma profiles of *Pseudogymnoascus*-species sample types in all possible combinations. The higher the PDI value, the lower the chemical relatedness between headspace volatiles of each possible paired combination. The *P. appendiculatus* strain (PA1) PCA mapping data cluster was most significantly different from *P. roseus* strain PR1, *P. destructans* strain PD3, and *P. pannorum* var. *pannorum* strain PP8, in decreasing order, based on mapping distance (between data clusters) and PDI (%). However, strain PA1 of *P. appendiculatus* was considerably less different (more chemically related) to *P. verrucosus* strain PV1, but moderately different from *P. destructans* strain PD6 as indicated by lower mapping distances and PDI values.

Strains PD3 and PD6 of *P. destructans* both indicated high levels of differences in PCA-mapping distance and PDIs from strain PP8 of *P. pannorum* var. *pannorum*. Strain PD3 also was highly different from *P. verrucosus* strain PV1, but only moderately

different from strain PR1 of *P. roseus* and PD6 of *P. destructans*. By contrast, strain PD6 had relatively low levels of differences in PCA-distance and PDIs from strain PR1 of *P. roseus* and strain PV1 of *P. verrucosus*.

Strain PP8 of P. *pannorum* var. *pannorum* showed high levels of differences in PCA-distance and PDIs with strain PR1 of *P. roseus* and strain PV1 of *P. verrucous. P. roseus* strain PR1 similarly showed a PCA mapping data cluster with very high significant differences in PCA-distances and PDI values from strain PV1 of *P. verrucosus.*

Construction of a 3-dimensional plot (aroma map) of all sample types tested using PCA provided a visual means of comparing the PCA mapping distances between data clusters of each sample type as well as an overall Discrimination Index (DI), indicating the relative overall strength or level of discrimination between all sample types included in the PCA test. Displayed DI values were validated by the Heracles II Alphasoft V14.20 software (using green highlighting), indicating a passing PCA test at P≤0.10 level of significance when a statistically-successful 3-D PCA-discrimination has been achieved between sample types (mapped data clusters).

The plotted aroma data cluster of *P. pannorum* var. *pannorum* strain PP8 was most obviously separated from the other fungi tested as indicated in the 3-dimensional PCA aroma map of fungal VOC-metabolite mixtures in culture headspace (Fig. 2). All of the *Pseudogymnoascus* species had data clusters that were highly separated from the SDA-culture control. The overall discrimination index (DI) was 65.0 for this 3-D PCA plot analysis.

Mapping data clusters in the 3-D PCA plot of e-nose aroma signature data among *Pseudogymnoascus* species were well separated with only a few minor overlaps for some combinations between species. Data clusters for *P. destructans* strains (red data clusters) were furthest or most distant from (least related) with *P. appendiculatus* strain PA1 and *P. pannorum* var. *pannorum* strain PP8, intermediately distant from (moderately related with) *P. verrucosus* strain PV1, and least distant from (most related to) *P. roseus* strain PR1. Thus, strain PV1 of *P. verrucosus* and strain PR1 of *P. roseus* were only moderately distant (more closely related) than any other data cluster pairs.

The percentages of total variance, accounting for the variability explained by each orthogonal principal component in the PCA, are as follows: PC 1 = 95.9 %; PC 2 = 2.9 %; and PC 3 = 0.6 %. Thus, most of the variability in the PCA was accounted for by PC 1 (x-axis), whereas PC 2 (y-axis) and PC 3 (z-axis) accounted for only a very small proportion of the total variance.

PCA distances, determined for each pairwise comparison of data clusters on the PCA-map and differences in aroma patterns, provided a means for visually displaying and quantifying differences that indicate levels of chemical relatedness between VOC-metabolite mixtures present in SDA-culture headspace of each *Pseudogymnoascus* species. This information, provided another metric of comparisons of chemical relatedness between pairs of strains of each species as shown in Fig. 3. These results, indicated by PCA distances (y-axis) relative to each strain pair, showed that the biggest differences in chemical relatedness between headspace volatiles (highest PCA distances), occurred (in order from highest to lower) for the data cluster pairs PD3-SDA, PP8-PD3, PA1-PD3, PD3-PV1, PR1-SDA, and PP8-PR1. The lowest PCA distances, indicating the least differences in chemical relatedness in VOC-metabolites, (in order from lowest to higher) were found between the data cluster pairs of PA1-PV1, PD6-PR1, (PP8-PA1, PP8-PV1, PP8-SDA all three equal), PP6-PV1, and (PA1-PD6, PV1-SDA both equal).

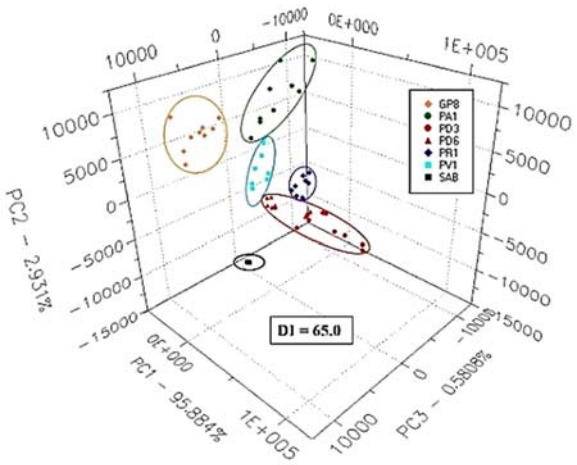

Fig. 2. PCA aroma map showing chemical relatedness between VOC-metabolites of five *Pseudogymnoascus* species produced in SDA-culture headspace. Symbols for figure caption of fungal strains: PA1 = *P. appendiculatus*, PD3, PD6 = *P. destructans*, PR1 = *P. roseus*, PV1 = *P. verrucosus*, GP8 (≡PP8) = *P. pannorum* var. *pannorum*, and SDA = Sabouraud dextrose agar (culture medium) control.

A further comparison-analysis of PCA distances between the strains of sample type pairs of different *Pseudogymnoascus* species provided some additional relevant information concerning chemical relatedness.

A pairwise comparison of PCA-distances between the two *P. destructans* strains (PD3-PD6), having a PCA-distance of approximately 56,000, to other combinations of these same Pd-strains with strains of four other *Pseudogymnoascus* species showed in five cases (i.e., PP8-PD6, PA1-PD6, PD3-PR1, PD6-PR1 and PD6-PV1) that the PCA-distances (17,400-46,600 range) were actually smaller than between Pd-strains. In contrast, PD3 had very large PCA-distances (81,100-101,300 range) with strains of *P. pannorum* var. *pannorum*, *P. appendiculatus*, and *P. verrucosus*, as indicated in the pairs PP8-PD3, PA1-PD3 and PD3-PV1.

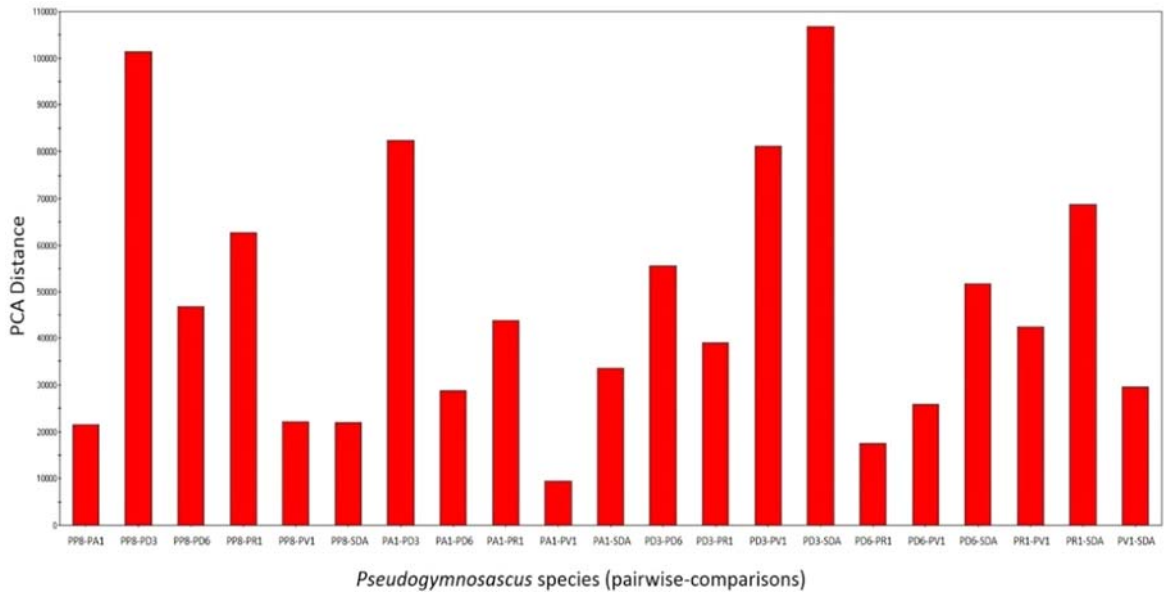

Fig. 3. PCA distances determined from pairwise-comparisons of VOC-profiles (smellprints) of volatile metabolites produced by five *Pseudogymnoascus* species in SDA-culture headspace. Symbols for *Pseudogymnoascus* strains: PA1 = *P. appendiculatus*, PD3, PD6 = *P. destructans* (WNS Pd-pathogen), PP8 = *P. pannorum* var. *pannorum*, PR1 = *P. roseus*, PV1 = *P. verrucosus*, and SDA = Sabouraud dextrose agar (culture medium) control.

4. Conclusions

Analyses of VOC profiles (peak patterns) from GC chromatograms of volatile metabolites produced in PDA-culture headspace indicated that all five of the *Pseudogymnoascus* species investigated appeared to produce some VOC metabolites in common, likely by using similar metabolic pathways by these genetically-related fungi. Differences in VOC peak heights at specific RTs provide further evidence that different *Pseudogymnoascus* species and strains may utilize slightly different metabolic pathways or variable gene expressions under identical cultural conditions to produce varying quantities of both common and different VOC-metabolites in culture headspace [21].

We are currently doing more extensive testing using various analytical methods to determine and confirm the identities and isomeric forms of all VOC-metabolites produced by *P. destructans*, and closely related fungi, which may be significant components of e-nose signatures useful for the noninvasive early detection of this pathogen and associated WNS-disease prior to symptom development. Nevertheless, preliminary tests here indicate the presence of normal oxidative- and fermentation-type catabolic products (ketones, aldehydes, and carboxylic acids), as well as some relatively low molecular weight volatile secondary metabolites from chemical classes common to other fungi. In particular, the probable production of monoterpenes and cyclic monoterpenes as major components of the complex VOC-metabolite mixtures released by strains of *P. destructans* in SDA-culture headspace provide evidence that this species utilizes one of the two main terpene (isoprene) biosynthesis pathways, specifically the mevalonic acid pathway, via dimethyl allyl diphosphate (DMAPP), isopentyl diphosphate (IPP), and geranyl diphosphate (GPP) intermediates to produce these volatile monoterpene secondary metabolites.

The primary carbon source in SDA medium is dextrose, a d-glucose aldohexose stereoisomer, which is readily utilized in catabolic pathways of microbes to produce a wide variety of metabolic products in nature. The use of dextrose by *P. destructans* to produce a diversity of VOC metabolic products from different chemical classes suggests that this fungus has a wide range of metabolic pathways available as an energy source and for production of secondary metabolites. Some of these metabolites, particularly the secondary metabolites, may be used as chemical defenses against other competing microbes present in the environment on carbon substrates utilized by the pathogen during its saprobic phase within hibernacula which serve as inoculum reservoirs of the fungus prior to pathogenic phases on bat hosts during winter hibernation periods.

Pseudogymnoascus pannorum var. *pannorum* produced two unique VOC-metabolites that were different from those produced by all other related fungal species tested. A previous, related study indicated that significant differences in VOC-metabolite mixtures produced in culture headspace in addition to pathogenicity differences, combined with PCA pairwise-comparisons and e-nose mapping data of VOC-metabolite mixtures, all suggest that *P. pannorum* and *P. pannorum* var. *pannorum* function metabolically as separate species [18].

The WNS Pd-pathogen was most closely related metabolically to *P. roseus* and *P. verrucosus*, and less related to *P. appendiculatus* based on 3-D PCA mapping distance, PDI, and data clustering on the e-

nose aroma map. These results were consistent with similar indications of relative genetic relatedness between these species based on genetic analyses using genomic DNA-homology tests [22].

One of the most significant results noted from PCA comparisons of aroma profiles was the discovery that the PCA-distance between *P. destructans* strains (PD3-PD6) was greater than some of the PCA-distances that were determined in pairwise comparisons between strains of the Pd-pathogen and other *Pseudogymnoascus* species. These results suggest that the metabolic pathways utilized by *P. destructans* strains from different geographic regions has diverged over time as the fungus has dispersed and become adapted to new environments, substrates, and bat hosts quite different from the conditions found in New York hibernacula where the pathogen was first introduced into North America. The mechanisms of metabolic changes in different sympatric Pd strains may be due to environmentally-induced effects on differential expression of metabolic genes or incrementally accumulated minor mutations in these genes over time and geographical space.

The uniquely different gaseous mixtures of VOC-metabolites produced in culture headspace by strains of *P. destructans*, compared to its non-pathogenic (saprophytic) cave-dwelling psychrophilic relatives, including *Geomyces* and other *Pseudogymnoascus* species common to cave sediments, indicate that the Pd-pathogen may have shifted its metabolic pathways toward pathogenic phenotypes and greater utilization of keratinogenic substrates. This possible metabolic shift in substrate specialization from saprobic to pathogenic phenotypes by *P. destructans* may have occurred at the expense of reduced saprotrophic enzyme activity [20]. Recent reports of reduced activity of urease and endoglucanase saprobic enzymes by *P. destructans* provide further evidence to suggest that this species may be shifting toward greater pathogenic activity [20, 23, 24].

Current methods and gold-standard criteria used for the definitive diagnosis of WNS in bats, since the beginning of the North American epizootic, involve destructive histological examinations (via wing-tissue thin sections under light microscopy) to detect the presence of curved Pd conidia and cupped epidermal lesions along with isolations or internal detections of *P. destructans* from infected skin tissue [25-27]. However, using purely histological methods is a problem for early WNS-disease detection because internal Pd-hyphae and epidermal erosions occur infrequently at early stages of infection, requiring euthanasia and extensive tissue sampling [28]. Other problems with current approaches to early disease detections include cases where: 1) the presence of Pd on bat skin does not necessarily lead to infection (depending on variable host susceptibility of different individuals and bat species), 2) Pd-infection does not result in WNS-disease development in all individuals and species, and 3) most current early-detection methods are either destructive or semi-destructive to bats in hibernation. The recent use of UV fluorescence for Pd-epidermal detections is noninvasive, but only indicates WNS-disease after small Pd-lesions (early symptoms) have already formed, thus not a true presymptomatic WNS-disease detection method at early stages of Pd-infection.

The acquisition of required skin swabs from bats for qPCR epidermal spore-load tests have significant effects on bat behavior and physiology due to potential arousals from torpor. This is especially true in cases when bats are handled and physically removed from cave walls or ceilings during swabbing (a common practice). Thus, skin swabs are considered semi-invasive and this possibility has led some researchers to swab alternative environmental substrates within bat roost sites to minimize disturbance to winter-hibernating bats [29, 30]. Furthermore, qPCR methods detect only low epidermal Pd-spore loads in presymptomatic bats (at very early stages of WNS-disease development prior to symptom development), precluding the use of this method for early disease detection since disease symptomology cannot be correlated with epidermal spore loads in early Pd-infections. There is also a high probability of false negative Pd-detections with qPCR at early Pd-infection stages due to sparse spore loads, requiring very high sampling rates. Some researchers have confused Pd-pathogen detection and DNA-quantification (on bat skins) with WNS-disease detection. This ideology ignores the many factors involved in Pd-infections of bats besides epidermal Pd-spore loads.

The need for truly non-invasive early WNS-disease detection and diagnostic methods becomes obvious with the additional requirement to prevent disturbance and arousal of bats during hibernation. Previous research provides strong evidence that arousals of bats from torpor states during winter hibernation periods may significantly reduce fat reserves and cause other physiological disturbances (e.g. severe dehydration) leading to starvation and reduced chances of winter survival [31-33].

The Heracles II GC/e-nose dual-technology instrument was effective in discriminating between genetically-related species of *Pseudogymnoascus*, based on the unique VOC-metabolite profiles present in SDA-culture headspace. Furthermore, PCA provided indications of differences in chemical relatedness between *Pseudogymnoascus* species based on unique mixtures of VOC-metabolites produced. The capability of e-nose devices to detect and discriminate between complex gaseous mixtures of VOC-metabolites produced by pathogenic and non-pathogenic keratinophilic fungi on bats could potentially provide part of the aroma signature (the fungal component) and first step necessary for developing a new noninvasive early detection method for diagnosing devastating wildlife diseases such as WNS. Cheaper, more portable e-nose devices potentially could be used to rapidly diagnose WNS in living bats and for determining the cause of death post-mortem [34, 35]. The WNS-epizootic already has killed an estimated seven million cave-swelling bats in

North America since the disease was first detected in New York State in 2006 [1, 36, 37]. The need for a rapid, noninvasive method for early WNS disease detection at the geographical advancing front of the epizootic is necessary to allow for applications of very early, more effective WNS-control applications, especially prior to the appearance of WNS-disease symptoms when treatments are most effective.

Acknowledgements

The authors thank Charisse Oberle for assistance in running Heracles II GC fast-gas/e-nose analyses of headspace volatiles from fungal cultures.

References

[1]. K. J. Vanderwolf, D. F. McAlpine, D. Malloch, G. J. Forbes, Ectomycota associated with hibernating bats in eastern Canadian caves prior to the emergence of White-nose Syndrome, *Northeastern Naturalist,* Vol. 20, Issue 1, 2013, pp. 115–130.

[2]. L. J. A. N. Johnson, A. N. Miller, R. A. McCleery, R. McClanahan, J. A. Kath, S. Lueschow, A. Porras-Alfaroa, Psychrophilic and psychrotolerant fungi on bats and the presence of *Geomyces* spp. on bat wings prior to the arrival of white nose syndrome*, Applied and Environmental Microbiology,* Vol. 79, Issue 18, 2013, pp. 5465–5471.

[3]. J. M. Lorch, A. M. Minnis, C. U. Meteyer, J. A. Redell, J. P. White, H. M. Kaarakka, L. K. Muller, D. L. Lindner, M. L. Verant, V. Shearn-Bochsler, D. S. Blehert, The fungus *Trichophyton redellii* sp. nov. causes skin infections that resemble white-nose syndrome of hibernating bats*, Journal of Wildlife Diseases,* Vol. 51, Issue 1, 2015, pp. 36-47.

[4]. US Fish and Wildlife Service, White-nose syndrome map 2017, USFWS, Hadley, Massachusetts (http://www.whitenosesyndrome.org/resources/map). Accessed 22 May 2017.

[5]. D. S. Blehert, A. C. Hicks, M. Behr, C. U. Meteyer, B. M. Berlowski-Zier, E. L. Buckles, J. T. H. Coleman, S. R. Darling, A. Gargas, R. Niver, J. C. Okoniewski, R. J. Rudd, W. B. Stone, Bat white-nose syndrome: an emerging fungal pathogen?, *Science*, Vol. 323, Issue 5911, 2009, p. 227.

[6]. G. R. Turner, D. M. Reeder, Update of white-nose syndrome in bats, *Bat Research News,* Vol. 50, Issue 3, 2009, pp. 47–53.

[7]. F. Courtin, W. B. Stone, G. Risatti, K. Gilbert, H. J. Van Kruiningen, Pathologic findings and liver elements in hibernating bats with white-nose syndrome, *Veterinary Pathology*, Vol. 47, Issue 2, 2010, pp. 214–219.

[8]. A. D. Wilson, D. G. Lester, C. S. Oberle, Development of conductive polymer analysis for the rapid detection and identification of phytopathogenic microbes, *Phytopathology*, Vol. 94, Issue 5, 2004, pp. 419–431.

[9]. A. D. Wilson, M. Baietto, Advances in electronic nose technologies developed for biomedical applications, *Sensors,* Vol. 11, Issue 1, 2011, pp. 1105-1176.

[10]. A. D. Wilson, M. Baietto, Applications and advances in electronic-nose technologies, *Sensors,* Vol. 9, Issue 7, 2009, pp. 5099-5148.

[11]. A. D. Wilson, Diverse applications of electronic-nose technologies in agriculture and forestry, *Sensors,* Vol. 13, Issue 2, 2013, pp. 2295–2348.

[12]. A. D. Wilson, Advances in electronic-nose technologies for the detection of volatile biomarker metabolites in the human breath, *Metabolites,* Vol. 5, Issue 1, 2015, pp. 140-163.

[13]. A. D. Wilson, Recent progress in the design and clinical development of electronic nose technologies, *Nanobiosensors in Disease Diagnosis*, Vol. 5, 2016, pp. 15-27.

[14]. C. Gianni, G. Caretta, C. Romano, Skin infection due to *Geomyces pannorum* var. *pannorum*, *Mycoses,* Vol. 46, Issue 9-10, 2003, pp. 430–432.

[15]. H. Zelenková, *Geomyces pannorum* as a possible causative agent of dermatomycosis and onychomycosis in two patients, *Acta Dermatovenerologica Croatica*, Vol. 14, Issue 1, 2006, pp. 21–25.

[16]. A. D. Wilson, Electronic-nose devices – potential for noninvasive early disease-detection applications, *Annals of Clinical Case Reports*, Vol. 2, Issue 1401, 2017, pp. 1-3.

[17]. A. D. Wilson, Finding aroma clues in the human breath to diagnose diseases, Atlas of Science (http://atlasofscience.org/finding-aroma-clues-in-the-human-breath-to-diagnose-diseases/) Accessed 29 February 2016.

[18]. A. D. Wilson, L. B. Forse, Discrimination between *Pseudogymnoascus destructans*, other dermatophytes of cave-dwelling bats, and related innocuous keratinophilic fungi based on electronic-nose/GC signatures of VOC-metabolites produced in culture, in *Proceedings of the 8th International Conference on Sensor Device Technologies and Applications (SENSORDEVICES' 2017)*, Rome, Italy, 10-14 September 2017, pp. 5-11.

[19]. R. S. Currah, Taxonomy of the Onygenales: Arthrodermataceae, Gymnoascaceae, Myxotrichaceae and Onygenaceae, *Mycotaxon*, Vol. 24, 1985, pp. 1–216.

[20]. H. T. Reynolds, H. A. Barton, Comparison of the white-nose syndrome agent *Pseudogymnoascus destructans* to cave-dwelling relatives suggests reduced saprotrophic enzyme activity, *PLoS ONE,* Vol. 9, Issue 1, 2014, e86437.

[21]. H. T. Reynolds, H. A. Barton, J. C. Slot, Phylogenomic analysis supports a recent change in nitrate assimilation in the white-nose syndrome pathogen, *Pseudogymnoascus destructans*, *Fungal Ecology*, Vol. 23, 2016, pp. 20-29.

[22]. A. M. Minnis, D. L. Lindner, Phylogenetic evaluation of *Geomyces* and allies reveals no close relatives of *Pseudomgymnoascus destructans*, comb. nov., in bat hibernacula of Eastern North America, *Fungal Biology*, Vol. 117, Issue 9, 2013, pp. 638-649.

[23]. M. Flieger, H. Bandouchova, J. Cerny, M. Chudíčková, M. Kolarik, V. Kovacova, N. Martínková, P. Novák, O. Šebesta, E. Stodůlková, J. Pikula, Vitamin B_2 as a virulence factor in *Pseudogymnoascus destructans* skin infection, *Scientific Reports*, Vol. 6, 2016, 33200.

[24]. H. T. Reynolds, T. Ingersoll, H. A. Barton, Modeling the environmental growth of *Pseudogymnoascus destructans* and its impact on the white-nose syndrome epidemic*, Journal of Wildlife Diseases,* Vol. 51, Issue 2, 2015, pp. 318-331.

[25]. C. U. Meteyer, E. L. Buckles, D. S. Blehert, A. C. Hicks, D. E. Green, V. Shearn-Bochsler,

N. J. Thomas, A. Gargas, M. J. Behr, Histopathologic criteria to confirm white-nose syndrome in bats, *Journal of Veterinary Diagnostic Investigations*, Vol. 21, 2009, pp. 411-414.

[26]. United States Geological Survey, National Wildlife Health Center (2014) Updated WNS case definitions. (http://www.whitenosesyndrome.org/resource/revised-case-definitions-white-nose-syndrome-11252014) Accessed 13 November 2017.

[27]. L. K. Muller, J. M. Lorch, D. L. Lindner, M. O'Connor, A. Gargas, D. S. Blehert, Bat white-nose syndrome: a real-time TaqMan polymerase chain reaction test targeting the intergenic spacer region of *Geomyces destructans*, *Mycologia*, Vol. 105, Issue 2, 2013, pp. 253-259.

[28]. L. P. McGuire, J. M. Turner, L. Warnecke, G. McGregor, T. K. Bollinger, V. Misra, J. T. Foster, W. F. Frick, A. M. Kilpatrick, C. K. R. Willis, White-nose syndrome disease severity and a comparison of diagnostic methods, *Ecohealth*, Vol. 13, Issue 1, 2016, pp. 60-71.

[29]. M. L. Verant, E. A. Bohuski, J. M. Lorch, D. S. Blehert, Optimized methods for total nucleic acid extraction and quantification of the bat white-nose syndrome fungus, *Pseudogymnoascus destructans*, from swab and environmental samples, *Journal of Veterinary Diagnostic Investigation*, Vol. 28, Issue 2, 2016, pp. 110-118.

[30]. J. M. Lorch, L. K. Miller, R. E. Russell, M. O'Connor, D. L. Lindner, D. S. Blehert, Distribution and environmental persistence of the causative agent of white-nose syndrome, *Geomyces destructans*, in bat hibernacula of the eastern United States, *Applied and Environmental Microbiology*, Vol. 79, Issue 4, 2013, pp. 1293-1301.

[31]. P. M. Cryan, C. Y. Meteyer, J. G. Boyles, D. S. Blehert, Wing pathology of white-nose syndrome in bats suggests life-threatening disturbances of physiology, *BMC Biology*, Vol. 8, 2010, p. 135.

[32]. D. M. Reeder, C. L. Frank, G. G. Turner, C U. Meteyer, A. Kurta, E. R. Britzke, M. E. Vodzak, S. R. Darling, C. W. Stihler, A. C. Hicks, R. Jacob, L. E. Grieneisen, S. A. Brownlee, L. K. Muller, D. S. Blehert, Frequent arousal from hibernation linked to severity of infection and mortality in bats with white-nose syndrome, *PloS ONE*, Vol. 7, Issue 6, 2012, e38920.

[33]. M. L. Verant, C. U. Meteyer, J. R. Speakman, P. M. Cryan, J. M. Lorch, D. S. Blehert, White-nose syndrome initiates a cascade of physiologic disturbances in the hibernating bat host, *BMC Physiology*, Vol. 14, 2014, p. 10.

[34]. A. D. Wilson, Biomarker metabolite signatures pave the way for electronic-nose applications in early clinical disease diagnoses, *Current Metabolomics*, Vol. 5, Issue 2, 2017, pp. 90-101.

[35]. A. D. Wilson, Electronic-nose applications in forensic science and for analysis of volatile biomarkers in the human breath, *Journal of Forensic Science and Criminology*, 1, S103, 2014, pp. 1-21.

[36]. A. Gargas, M. T. Trest, M. Christensen, T. J. Volk, D. S. Blehart, *Geomyces destructans* sp. nov. associated with bat white-nose syndrome, *Mycotaxon*, Vol. 108, Issue 1, 2009, pp. 147-154.

[37]. J. M. Lorch, C. U. Meteyer, M. J. Behr, J. G. Boyles, P. M. Cryan, A. C. Hicks, A. E. Ballmann, J. T. H. Coleman, D. N. Redell, D. M. Reeder, D. S. Blehert, Experimental infection of bats with *Geomyces destructans* causes white-nose syndrome, *Nature*, Vol. 480, Issue 7377, 2011, pp. 376-378.